

https://doi.org/10.1070/QEL16997

Formation of spectra of saturated-absorption resonances on closed transitions in the spectroscopy of unidirectional waves

E.G. Saprykin, A.A. Chernenko

Abstract. **The formation of spectra of saturated-absorption resonances on the atomic transitions with level momenta $J = 0 \rightarrow J = 1$ and $J = 1 \rightarrow J = 2$ are investigated, both numerically and analytically, by the method of unidirectional linearly polarised laser waves in order to determine how the transition openness (radiation branching) affects these spectra. It is shown that, along with quantitative changes, determined by the relaxation constants of levels, value of their splitting, polarisation orientation, and wave intensities, the spectra undergo qualitative changes with a change in the degree of atomic transition openness.**

Keywords: *saturated-absorption resonance, unidirectional waves, closed and open transitions.*

1. Introduction

Nonlinear spectroscopic effects occurring in atomic media upon resonance interaction with laser fields are the main tool of laser spectroscopy, which provides information about the characteristics of these objects when other techniques are inaccessible (in particular, in the case of cold atoms) and use them in practical applications. An especially important and interesting class of nonlinear effects is related to the coherence of atomic states during two-photon processes, which manifests itself in the form of narrow spectral structures. Despite the fact that the occurrence of coherence of atomic states during two-photon transitions had been known even in the pre-laser times, the discovery of lasers made it possible to intensify significantly the study of these coherent phenomena (see, e.g., review [1]). Later on the resonances caused by the coherence of atomic states in the presence of laser radiation were referred to as electromagnetically induced transparency (EIT) resonances and electromagnetically induced absorption (EIA) resonances. Many phenomena revealed then were 'rediscovered' and renamed in the studies devoted to EIT and EIA. This issue, as well as the mistakes in interpreting a number of results obtained in that period, were enlightened in the introduction to our work [2].

An example of coherent phenomena on atomic transitions from the ground state are EIT resonances [3], which are based on coherent population trapping (CPT) for levels [4]. However, along with them, resonances with opposite sign (EIA resonances) were also revealed on these transitions. These resonances were recorded for the first time specifically in the field of two unidirectional laser waves with close frequencies on a closed transition in the Rb atom [5]. They were explained by the spontaneous transfer of the magnetic coherence of the excited state levels to the ground state under conditions of a closed transition [6]. Thereafter EIA resonances were also observed on a number of other transitions from the ground state of the Rb and Cs atoms [7]. Later on, the detection (with the aid of magnetic scanning) of EIT and EIA resonances in the field of two counterpropagating laser waves was reported in [8]. The experimentally observed behavioural features of the of EIA resonances on degenerate transitions could not always be explained within the mechanism proposed in [6] (see, e.g., [7, 8]). Therefore, other processes (not always justified but yielding resonance structures similar to experimental ones) were also considered. Examples are optical pumping and CPT [7], as well as collisions [9].

Nevertheless, it was stated recently in [10], in the development of the concept proposed in [6], that the formation of narrow structures in the spectra of saturated-absorption (EIA) resonance on closed transitions with an arbitrary value of total level momenta is specifically the spontaneous transfer of the magnetic coherence of upper state levels, induced by light fields, to a lower state. At the same time, we did not analyse in this study any other processes that could lead to the formation of narrow nonlinear resonance structures were analysed.

It was shown in [11] that, in the case of a simple two-level system, the form of narrow nonlinear resonance structures in the field of two unidirectional waves depends on the degree of atomic transition openness. Specifically, the structure manifests itself as EIT and EIA resonances on closed and open transitions, respectively. These structures arise due to the coherent beatings of transition level populations in the two-frequency field.

An investigation [12] of the physical processes of EIA spectrum formation and probe-wave magnetic scanning on open and closed transitions between levels with a total momentum $J = 1$ in the case of unidirectional waves showed that narrow saturated-absorption resonance structures on these transitions are formed in the Λ schemes. In the cases of parallel and orthogonal field polarisations, they are determined, respectively, by the coherent beatings of level populations [11] and nonlinear interference effect [13]. Here, even when the upper state is closed, the two-level transitions between magnetic sublevels turn out to be open, which leads, according to [11], to the formation of a narrow structure in the form of an EIT resonance. The level magnetic coherence forms EIT and EIA resonances in the magnetic scanning spectra. The main

E.G. Saprykin Institute of Automation and Electrometry, Siberian Branch, Russian Academy of Sciences, prosp. Akad. Koptyuga 1, 630090 Novosibirsk, Russia; e-mail: edgenych@ngs.ru;
A.A. Chernenko Rzhanov Institute of Semiconductor Physics, Siberian Branch, Russian Academy of Sciences, prosp. Akad. Lavrent'eva 13, 630090 Novosibirsk, Russia; e-mail: chernen@isp.nsc.ru

Received 12 March 2019
Kvantovaya Elektronika **49** (5) 479–487 (2019)
Translated by Yu.P. Sin'kov

contribution is from the magnetic coherence of the lower state levels, whereas the contribution of spontaneous coherence transfer from the upper state levels to the lower state is small and manifests itself only quantitatively. The results of [12] are also valid for the transitions of the $J \to J$ and $J \to J-1$ types, because resonance spectra are also formed on these transitions in the Λ schemes. Another situation is with the $J \to J+1$ transitions, where, because of the oscillator strength ratio between the magnetic sublevels, the main contribution to the resonance spectrum is from the V schemes, which are formed by the sublevels with the maximum number M. Closed two-level transitions, in which the form of narrow structures depends basically on the atomic transition openness, are formed specifically in the V schemes [11]. In this context, of interest are atoms with the ground state $^1S_0$ (alkali-earth and similar atoms), in which a closed V scheme is implemented on the resonance transition ($J = 0 \to J = 1$) in a dual-frequency optical field.

The purpose of this study is to analyse the formation of EIA resonances in the method of the probe field of unidirectional laser waves on closed atomic transitions with level momenta $J = 0 \to J = 1$ and $J = 1 \to J = 2$ in order to determine the role of the transition openness in the formation of these resonances.

2. Theoretical model

Let us consider the problem about the absorption spectrum of a probe field in a gas of atoms on the transitions between the levels with the momenta $J = 0 \to J = 1$ (V-type transition) or $J = 1 \to J = 2$ in the field of a strong unidirectional wave. These transitions are schematically shown in Fig. 1. The strong wave is assumed to be plane, monochromatic, linearly polarised (frequency ω, wave vector $\boldsymbol{k}$, electric field strength $\boldsymbol{E}$), and resonant with the $m \to n$ transition (transition frequency ω_{mn}). The probe wave is also monochromatic (frequency ω_μ, wave vector $\boldsymbol{k}_\mu$, electric field strength $\boldsymbol{E}_\mu$), with circular (for the V scheme) or linear polarisation, parallel or orthogonal to the strong-field polarisation. It is assumed that the medium is placed in a magnetic field with a strength $\boldsymbol{H}$, whose value may change, and the wave propagates in the magnetic field direction. The problem is solved taking into account that the medium is saturated by the probe wave (on the assumption that it is weak as compared with the strong wave). The gas is assumed to be dilute; hence, collisions can be neglected. The medium is considered to be optically thin.

The problem will be solved in a coordinate system with a quantisation axis directed along the vector $\boldsymbol{H}$ ($\boldsymbol{H} \parallel$ оси Z). Transitions with a change in the magnetic quantum number $\Delta M = \pm 1$ are allowed for fields in this coordinate system. According to Fig. 1b, Λ and V subsystems are formed on the $J = 1 \to J = 2$ transition; these subsystems are coupled by spontaneous processes.

When solving the problem, we proceeded from the equations for the density matrix of the atomic system. According to [13], the dynamics of diagonal elements ρ_i and off-diagonal elements ρ_{ik} of the density matrix in the relaxation-constant model is described by the system of equations

$$\frac{\mathrm{d}\rho_i}{\mathrm{d}t} + \Gamma_i\rho_i = Q_i + \sum_k A_{ki}\rho_k - 2\,\mathrm{Re}\left(\mathrm{i}\sum_j V_{ij}\rho_{ji}\right) - 2\,\mathrm{Re}\left(\mathrm{i}\sum_j V^\mu_{ij}\rho_{ji}\right), \quad (1)$$

$$\frac{\mathrm{d}\rho_{ik}}{\mathrm{d}t} + (\Gamma_{ik} + \mathrm{i}\omega_{ik})\rho_{ik} = -\,\mathrm{i}[V,\rho]_{ik} - \mathrm{i}[V^\mu,\rho]_{ik} + R^{(2)}_{ik}. \quad (2)$$

Here, the total derivative operator $\mathrm{d}/\mathrm{d}t = \partial/\partial t + \boldsymbol{v}\nabla$ ($\boldsymbol{v}$ is the atomic velocity vector); Γ_i are the level relaxation constants; Γ_{ik} are the transition half-widths; Q_i are the level excitation rates; and V and V^μ are, respectively, the atomic interaction operators with strong and probe fields: $V = -G\exp(\mathrm{i}(\boldsymbol{kr} - \omega t)) + \mathrm{h.c.}$, and $V^\mu = -G^\mu\exp(\mathrm{i}(\boldsymbol{k}_\mu\boldsymbol{r} - \omega_\mu t)) + \mathrm{h.c.}$, where $G = \boldsymbol{dE}/2\hbar$, $G^\mu = \boldsymbol{dE}_\mu/2\hbar$, and $\boldsymbol{d}$ is the dipole moment operator. The terms $A_{ki}\rho_k$ in Eqn (1) determine the spontaneous population decay. The term $R^{(2)}_{ik}$ in Eqn (2) describes the spontaneous transfer of magnetic coherence from the upper state levels to the lower state (this term is absent in the equations for the V-type transition). The quantity $a_0 = A_{mn}/\Gamma_m \leqslant 1$, referred to as the branching ratio, plays an important role in the formation of resonance spectra. For open and closed transitions, $a_0 < 1$ and $a_0 = 1$, respectively.

Note that this statement of problem and solution are valid for both the transitions between excited states and in the case where the lower state n is the ground state of atom. The relax-

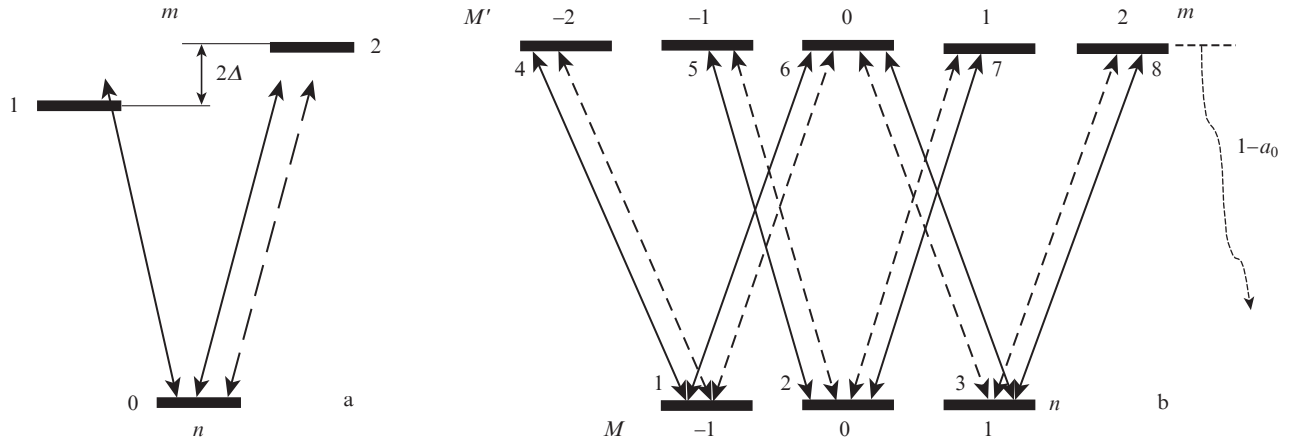

Figure 1. Schematic diagram of the interaction of optical fields with the sublevels of the $J = 0 \to J = 1$ and $J = 1 \to J = 2$ transitions (the solid and dashed lines show strong and probe fields, respectively; $1 - a_0$ is the fraction of spontaneous decay of sublevels of the m state to other lower levels).

ation constant of the lower level is determined by the ensemble-average time of particles interaction with the light field.

Solutions to the system of equations (1), (2) for the density matrix will be sought in the following form: diagonal elements $\rho_i = \rho_i^0 + \rho_i^+ \exp[\mathrm{i}(\varepsilon t - (\boldsymbol{k}_\mu - \boldsymbol{k})\boldsymbol{r})] + \rho_i^- \exp[-\mathrm{i}(\varepsilon t - (\boldsymbol{k}_\mu - \boldsymbol{k})\boldsymbol{r})]$ and off-diagonal elements $\rho_{ik} = R_{ik}\exp(-\mathrm{i}(\omega t - \boldsymbol{k}\boldsymbol{r})) + R_{ik}^\mu \exp(-\mathrm{i}(\omega_\mu t - \boldsymbol{k}_\mu \boldsymbol{r})) + R_{ik}^\mathrm{s} \exp(-\mathrm{i}(\omega_\mathrm{s} t - \boldsymbol{k}_\mathrm{s}\boldsymbol{r}))$ (allowed transitions) or $\rho_{ik} = r_{ik}^0 + r_{ik}^+ \exp[\mathrm{i}(\varepsilon t - (\boldsymbol{k}_\mu - \boldsymbol{k})\boldsymbol{r})] + r_{ik}^- \exp[-\mathrm{i}(\varepsilon t - (\boldsymbol{k}_\mu - \boldsymbol{k})\boldsymbol{r})]$ (forbidden transitions), where $\varepsilon = \omega_\mu - \omega$, $\omega_\mathrm{s} = 2\omega - \omega_\mu$, and $\boldsymbol{k}_\mathrm{s} = 2\boldsymbol{k} - \boldsymbol{k}_\mu$. The validity of this form of solutions in a wide range of transition parameters was shown in [14].

2.1. $J = 0 \to J = 1$ transition

For this transition (see Fig. 1a), Eqns (1) yield in the stationary case the following system of equations describing the populations of the lower (0) and upper (1, 2) levels:

$$\Gamma_n \rho_0^0 = Q_0 + \sum_{k=1,2} A_{k0}\rho_k^0 + \sum_{k=1,2} 2\,\mathrm{Re}(\mathrm{i}G_{0k}R_{k0}) + 2\,\mathrm{Re}(\mathrm{i}G_{02}^\mu R_{20}^\mu), \tag{3a}$$

$$(\Gamma_n + \mathrm{i}\varepsilon)\rho_0^+ = \sum_{k=1,2} A_{k0}\rho_k^+ + \mathrm{i}(G_{01}R_{10}^\mathrm{s} + G_{02}R_{20}^\mathrm{s}) + \mathrm{i}(G_{02}^\mu R_{20} - G_{20}R_{02}^\mu - G_{10}R_{01}^\mu), \tag{3b}$$

$$\Gamma_m \rho_1^0 = Q_1 + 2\,\mathrm{Re}(\mathrm{i}G_{10}R_{01}), \tag{3c}$$

$$(\Gamma_m + \mathrm{i}\varepsilon)\rho_1^+ = \mathrm{i}(G_{10}R_{01}^\mu - G_{01}R_{10}^\mathrm{s}), \tag{3d}$$

$$\Gamma_m \rho_2^0 = Q_2 + 2\,\mathrm{Re}(\mathrm{i}G_{20}R_{02}) + 2\,\mathrm{Re}(\mathrm{i}G_{20}^\mu R_{02}^\mu), \tag{3e}$$

$$(\Gamma_m + \mathrm{i}\varepsilon)\rho_2^+ = \mathrm{i}(G_{20}R_{02}^\mu - G_{02}^\mu R_{20} - G_{02}R_{20}^\mathrm{s}). \tag{3f}$$

Correspondingly, the systems of equations for the polarisations on the allowed ($1 \to 0$, $2 \to 0$) and forbidden ($2 \to 1$) transitions can be written as

$$(\Gamma_{mn} + \mathrm{i}\Omega_{10})R_{01} = \mathrm{i}G_{01}(\rho_1^0 - \rho_0^0) + \mathrm{i}G_{02}r_{21}^0 + \mathrm{i}G_{02}^\mu r_{21}^-, \tag{4a}$$

$$(\Gamma_{mn} + \mathrm{i}(\Omega_{10} - \varepsilon))R_{01}^\mathrm{s} = \mathrm{i}G_{01}(\rho_1^- - \rho_0^-) + \mathrm{i}G_{02}r_{21}^-, \tag{4b}$$

$$(\Gamma_{mn} + \mathrm{i}\Omega_{10}^\mu)R_{01}^\mu = \mathrm{i}G_{10}(\rho_1^+ - \rho_0^+) + \mathrm{i}G_{02}r_{21}^+ + \mathrm{i}G_{02}^\mu r_{21}^0; \tag{4c}$$

$$(\Gamma_{mn} - \mathrm{i}\Omega_{20})R_{20} = -\mathrm{i}G_{20}(\rho_2^0 - \rho_0^0) - \mathrm{i}G_{20}^\mu(\rho_2^+ - \rho_0^+) - \mathrm{i}G_{10}r_{21}^0, \tag{4d}$$

$$(\Gamma_{mn} - \mathrm{i}(\Omega_{20} - \varepsilon))R_{20}^\mathrm{s} = -\mathrm{i}G_{20}(\rho_2^+ - \rho_0^+) - \mathrm{i}G_{10}r_{21}^+, \tag{4e}$$

$$(\Gamma_{mn} - \mathrm{i}\Omega_{20}^\mu)R_{20}^\mu = -\mathrm{i}G_{20}(\rho_2^+ - \rho_0^+) - \mathrm{i}G_{20}^\mu(\rho_2^0 - \rho_0^0) - \mathrm{i}G_{10}r_{21}^-; \tag{4f}$$

$$(\Gamma_{21} + \mathrm{i}\omega_{21})r_{21}^0 = \mathrm{i}(G_{20}R_{01} - G_{01}R_{20} + G_{20}^\mu R_{01}^\mu), \tag{5a}$$

$$(\Gamma_{21} + \mathrm{i}(\omega_{21} + \varepsilon))r_{21}^+ = \mathrm{i}(G_{20}R_{01}^\mu - G_{01}R_{20}^\mathrm{s}), \tag{5b}$$

$$(\Gamma_{21} + \mathrm{i}(\omega_{21} - \varepsilon))r_{21}^- = \mathrm{i}(G_{20}^\mu R_{01} - G_{01}R_{20}^\mu + G_{20}R_{01}^\mathrm{s}). \tag{5c}$$

The quantities Γ_n and Γ_m in Eqns (3)–(5) are, respectively, the relaxation constants of the lower (n) and upper (m) levels; Γ_{mn} is the transition line half-width; Γ_{21} is the polarisation relaxation constant between the magnetic sublevels of the upper state (magnetic coherence); and $\Omega_{ik} = \omega - \omega_{ik}$ and $\Omega_{ik}^\mu = \omega_\mu - \omega_{ik}$ are the frequency detunings of the strong and probe fields from the frequencies ω_{ik} of the transitions between the m and n sublevels. We assume the level populations in the absence of fields to be $\rho_0 = N_n$ and $\rho_1 = \rho_2 = N_m$.

The consideration of atomic motion is reduced to the replacements $\Omega_{ik} \to \Omega_{ik} - \boldsymbol{k}\boldsymbol{v}$, $\Omega_{ik}^\mu \to \Omega_{ik}^\mu - \boldsymbol{k}_\mu\boldsymbol{v}$, and $\varepsilon \to \varepsilon - (\boldsymbol{k}_\mu - \boldsymbol{k})\boldsymbol{v}$ in the equations. Below we consider the cases of unidirectional ($\boldsymbol{k} \approx \boldsymbol{k}_\mu$) waves with close frequencies.

The shape of the probe field absorption line (per atom) was determined as

$$\alpha/(\alpha_0 N_{nm}) = -\Gamma_{mn}\langle \mathrm{Re}(\mathrm{i}\,(R_{20}^\mu G_{02}^\mu))/|\,G^\mu\,|^2\rangle, \tag{6}$$

where $\langle ... \rangle$ means averaging over the Maxwellian distribution of particle velocities and $\alpha_0 = 4\pi\omega_{mn}d^2/c\hbar\Gamma_{mn}$ is the resonance absorption cross section. The probabilities A_{ki} of the spontaneous decay of magnetic sublevels in each channel were assumed to be identical and equal to A_{mn}.

Since the exact analytical solutions to the steady-state system of equations (3)–(5) are complicated and low-informative, these equations were solved numerically. To reveal the physical processes responsible for the structural features of resonance spectra, analytical solutions to this system of equations were obtained in some cases in the approximation of weak probe field and first nonlinear corrections for the strong field. Numerical calculations of the $J = 0 \to J = 1$ and $J = 1 \to J = 2$ transitions (see below) were performed with the following values of relaxation constants: $\Gamma_m = 5.5 \times 10^7$ s^{-1}, $\Gamma_n = (10^{-2}-10^{-1})\Gamma_m$, $\Gamma_{mn} = (\Gamma_m + \Gamma_n)/2$, $\Gamma_{21} = \Gamma_m$, and $A_{mn} = a_0\Gamma_m$. In the case of resonance transition, the branching ratio $a_0 = 1$, because the upper state decay occurs on the working (closed) transition. For the transitions from the ground to excited states or between excited states, the parameter $a_0 < 1$ (open transitions), because there are channels of spontaneous decay of the upper working level to lower levels. The Doppler linewidth kv_T was assumed to be 5.2×10^9 s^{-1}, the range of variation in the particle velocities in the integration was $\pm 3kv_\mathrm{T}$ with a step $\Delta kv_\mathrm{T} = (10^{-3}-10^{-4})kv_\mathrm{T}$. The saturation parameters of the strong (κ_s) and probe (κ_p) fields were determined as $\kappa_\mathrm{s} = 2(dE/2\hbar)^2\gamma_{mn}/(\Gamma_{mn}\Gamma_m\Gamma_n)$ and $\kappa_\mathrm{p} = 2(dE_\mu/2\hbar)^2\,\gamma_{mn}/(\Gamma_{mn}\Gamma_m\Gamma_n)$, where E and E_μ are, respectively, the strengths of the circular components of strong and probe fields; d is the reduced transition dipole moment; and $\gamma_{mn} = \Gamma_m + \Gamma_n - A_{mn}$. The values of saturation parameters were varied in the ranges $\kappa_\mathrm{s} \leqslant 50$ and $\kappa_\mathrm{p} \leqslant \kappa_\mathrm{s}$.

The results of numerical calculations of the saturated absorption shape for a circularly polarised probe wave are presented for closed (Fig. 2a) and open ($a_0 = 0.5$) (Fig. 2b) $J = 0 \to J = 1$ transitions at $\Omega_\mathrm{s} = 0$, $\Gamma_n = 0.02\Gamma_m$, $\kappa_\mathrm{s} = 1$, $\kappa_\mathrm{p} = 10^{-3}$, and several splittings of upper state levels. In the absence of level splitting, a resonance is formed on the Doppler profile of the probe-wave absorption line near the frequency detuning $\Omega_\mu = 0$. The resonance profile is a conventional wide hole with a narrow small-amplitude structure at the line centre [curves (*1*)]. This structure manifests itself as a narrow absorption peak for a closed transition and as a narrow transmission peak for open transitions. The resonance shapes are determined in this case by the contributions of the processes

occurring in two- and three-level transition schemes. If the level splittings exceed the transition width ($\Delta > \Gamma_{mn}$), the resonances formed in the two- and three-level schemes become frequency-separated and manifest themselves in the pure form [curves (*2*) and (*3*)]. In the two-level system (levels 0 and 2), a resonance is formed by wave fields with identical circular polarisations. This resonance arises near the field frequency difference $\varepsilon = \omega_\mu - \omega = 0$ and manifests itself as a conventional population hole. The hole centre at $\varepsilon = 0$ is characterised (as in the absence of level splitting) by the presence of a narrow absorption peak for a closed transition or a transmission peak for an open transition (see Fig. 2). In a three-level system, a resonance is formed by fields with different circular polarisations. It arises near $\varepsilon = \omega_\mu - \omega = \omega_{21} = 2\Delta$ and also manifests itself as a hole but with other parameters. Note that the hole profiles for closed and open transitions differ in both amplitude and width, as well as in the shape of wings: maxima characteristic of coherent processes are formed in the wings for a closed transition, whereas an open transition exhibits no such structures.

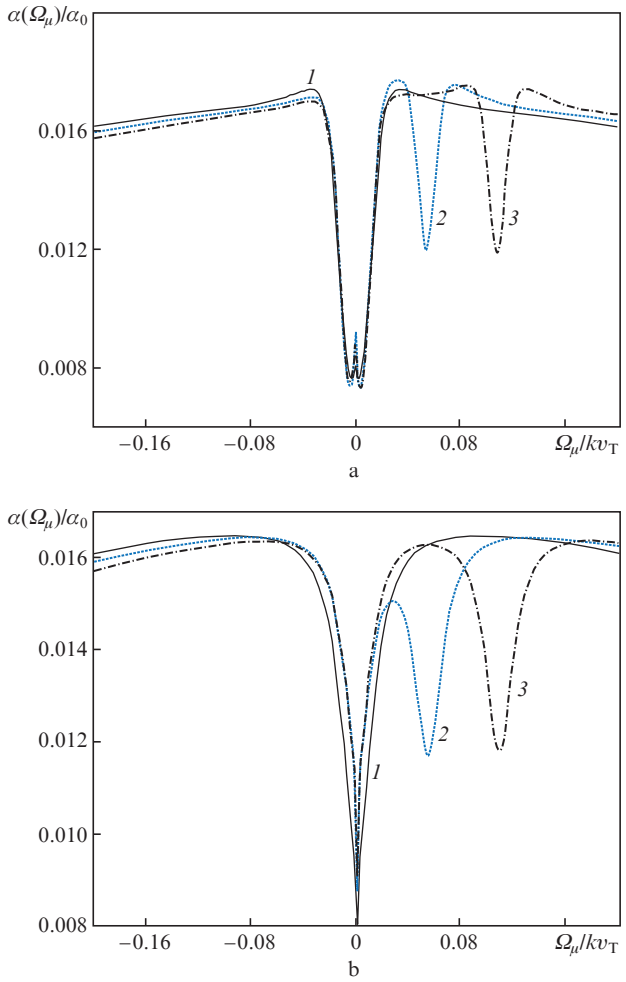

Figure 2. Shapes of the resonances on the (a) closed and (b) open ($a_0 = 0.5$) $J = 0 \to J = 1$ transitions at $\Omega_s = 0$, $\kappa_s = 1$, $\kappa_p = 10^{-2}$, $\Gamma_n = 0.02\Gamma_m$; and different upper state splittings: $\Delta = (1)\ 0$, $(2)\ 5\Gamma_{mn}$, and $(3)\ 10\Gamma_{mn}$.

The influence of the strong field intensity on the shape of the saturated absorption line of the probe wave on a closed transition is shown in Fig. 3; the saturation parameter κ_s ranges from 0.002 to 0.1. Under these conditions, a rise in the strong-wave intensity leads to a linear increase in the amplitudes of both holes and the peak structure amplitude, but affects only slightly the width of the holes and structures. For example, the central hole amplitude exceeds the shifted-hole amplitude by a factor of 2–2.5 and the peak-structure amplitude by a factor of 3–4. The hole widths change by about 20%, whereas no changes in the width of the peak structure were found. Note that a rise in the strong-field intensity leads to a qualitative change in the shape of the frequency-shifted resonance: wide peaks arise in the hole wings [curves (*4–6*)] at $\kappa_s > 0.01$, whose amplitudes and widths, as well as the positions of maxima, depend on the κ_s value.

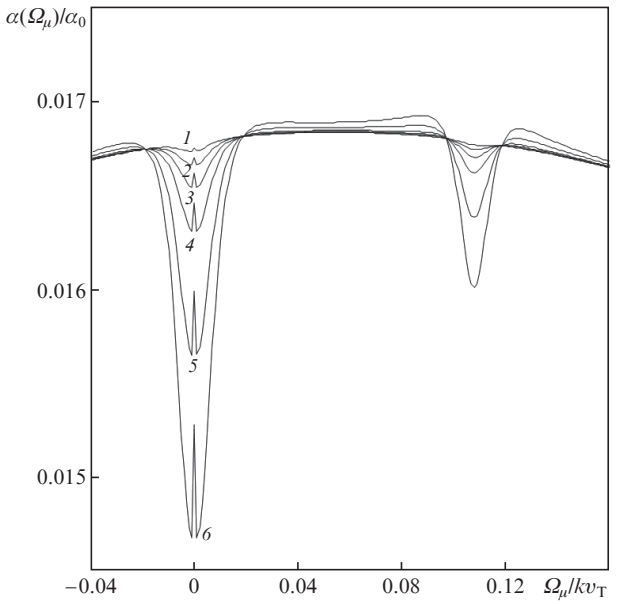

Figure 3. Shape of the resonance on a closed $J = 0 \to J = 1$ transition at $\Omega_s = 0$, $\Gamma_n = 0.02\Gamma_m$, $\Delta = 10\Gamma_{mn}$, $\kappa_p = 10^{-3}$; and different strong-wave saturation parameters: $\kappa_s = (1)\ 2\times10^{-3}$, $(2)\ 5\times10^{-3}$, $(3)\ 10^{-2}$, $(4)\ 2\times10^{-2}$, $(5)\ 5\times10^{-2}$, and $(6)\ 10^{-1}$.

Analytical calculations showed that the lower level undergoes a field splitting at saturation parameters $\kappa_s > 0.01$; this splitting leads to the observed change in the resonance shape. When $\kappa_s > 0.5$, the dependences of the central-hole amplitude and width become root-like, whereas the rise in the shifted-hole amplitude remains linear. The shifted-hole width rises nonlinearly but slower than that of the central hole. A rise in the strong-wave intensity leads to an increase in the amplitudes and widths of the peaks in the shifted-hole wings and an increase in the distance between their maxima; the corresponding dependences on intensity are root-like. The peak-structure amplitude also changes nonlinearly and reaches a maximum at $\kappa_s = 1–2$. The maximum peak-to-hole contrast is $\sim 30\%$; it is implemented at $\kappa_s \approx 0.5–0.7$. A change in the strong-wave intensity does not affect the peak width.

Calculations of the shape of nonlinear resonance on the open transition (at $a_0 = 0.5$) showed that the amplitude and width of the holes formed in two- and three-level systems in the range of $\kappa_s \sim 10^{-2}–50$ are identical and depend identically on κ_s: the amplitudes rise linearly at $\kappa_s < 1$ and according to the root law at $\kappa_s \gg 1$, while the dependences of the width are root-like in the entire range.

The dependence of the narrow structure (hole) amplitude on the saturation parameter κ_s, as in the case of closed transition, is also nonlinear, with a maximum in the vicinity of $\kappa_s \sim 2$. The narrow-structure contrast with respect to the hole reaches a maximum (almost 100%) at small κ_s values (~ 0.1). The contrast of the structure decreases with an increase in κ_s. However, for an open transition, in contrast to a closed one, a rise in the parameter κ_s in the range of 0^{-2}–10 leads to an increase in the narrow-structure width by more than twice.

Numerical and analytical calculations showed that the parameters of resonance narrow structures (peak and hole) are determined by the lower level relaxation constant Γ_n. A decrease in Γ_n leads to a rise in the amplitudes of narrow structures and a decrease in their widths. This effect should manifest itself upon cooling an atomic ensemble.

2.2. Analytical solutions for the V scheme

To reveal the physical processes responsible for the structure of EIA resonance spectra (see Figs 2, 3), we will consider the approximate solutions of the system for two- and three-level transitions.

In a system having two levels (0 and 2, Fig. 1a), the resonance shape can be derived from Eqns (3)–(5) for a weak probe field, in the approximation of the first nonlinear strong-field corrections and large Doppler broadening ($\Gamma_{mn} \ll kv_T$), in the form [11]

$$\frac{\alpha(\varepsilon)}{\alpha_0 N_{nm}} = \sqrt{\pi}\frac{\Gamma_{mn}}{kv_T}\exp\left[-\left(\frac{\Omega_\mu}{kv_T}\right)^2\right]\left\{1 - 2|G|^2\,\mathrm{Re}\left[\frac{1}{2\Gamma_{mn} - i\varepsilon}\right.\right.$$
$$\left.\left.\times\left(\frac{\Gamma_m + \Gamma_n - A_{mn}}{\Gamma_m\Gamma_n} + \frac{a_m}{\Gamma_m - i\varepsilon} + \frac{a_n}{\Gamma_n - i\varepsilon}\right)\right]\right\}, \qquad (7)$$

where

$$a_m = \frac{\Gamma_m + A_{mn} - \Gamma_n}{\Gamma_m - \Gamma_n}, \quad a_n = \frac{\Gamma_m - A_{mn} - \Gamma_n}{\Gamma_m - \Gamma_n}.$$

It follows from expression (7) that a resonance consisting of three spectral components with different widths and amplitudes is formed in the probe-wave absorption spectrum near the frequency detunings $\varepsilon = 0$ ($\Omega_\mu = \Omega$). The component described by the first term in the nonlinear part of (7) is due to the strong-field saturation; it forms a conventional population hole with a half-width $2\Gamma_{mn}$ in the spectrum. The other two components (the second and third terms) are due to the level population beatings and have half-widths Γ_m and Γ_n, respectively. The component amplitudes are determined by the coefficients a_m and a_n. It follows from the expressions for the coefficients that the sign of a_n depends on the relationship between the relaxation constants and Einstein coefficient A_{mn}. The narrow structure manifests itself in the spectrum as an additional hole ($a_n > 0$) when the constants are related as $\Gamma_m > \Gamma_n$ and $\Gamma_m - A_{mn} > \Gamma_n$ and in the form of a peak ($a_n < 0$) when $\Gamma_m - A_{mn} < \Gamma_n$ the narrow structure is absent in the resonance spectrum, because $a_n = 0$ in this case.

For a long-lived lower level ($\Gamma_m \gg \Gamma_n$), we have

$$a_m \approx \frac{\Gamma_m + A_{mn}}{\Gamma_m} = 1 + a_0,$$

$$a_n \approx \frac{\Gamma_m - A_{mn} - \Gamma_n}{\Gamma_m} = 1 - a_0 - \frac{\Gamma_n}{\Gamma_m},$$

where $a_0 = A_{mn}/\Gamma_m$ is the radiation branching ratio. For the transitions with the parameter $a_0 < 1 - \Gamma_n/\Gamma_m$ (i.e., open transitions), it follows from expression (7) that the probe-wave absorption line is shaped as a wide hole with a half-width $2\Gamma_{mn}$ and a narrow hole with a half-width Γ_n within the wide one; the amplitudes of narrow and wide holes are identical. Specifically this amplitude relationship is observed in numerical calculations of resonance shapes for open transition at small saturation parameters ($\kappa_s \leqslant 0.1$).

At the a_0 values in range of $1 - \Gamma_n/\Gamma_m < a_0 \leqslant 1$ the transition is closed. In this case the absorption line profile looks like a wide (with a half-width $2\Gamma_{mn}$) hole, within which a narrow absorption peak with a half-width Γ_n is formed. The narrow peak amplitude is smaller than the hole amplitude by a factor of about 3, which is in agreement with the numerical calculation data on the peak contrast at small saturation parameters κ_s.

Note that in the approximation of first nonlinear corrections the amplitudes of the main hole and narrow structures of the resonance depend linearly on the strong field intensity, whereas the widths of the hole and its structures are independent of the field intensity. This fact was noted above when discussing the numerical calculation results presented in Fig. 3. With allowance for the next strong-field corrections, the dependences of the parameters of the main hole (see [13]) and its narrow structures [15] on the strong field intensity behave differently. When the constants are related as $\Gamma_n \ll \Gamma_m$, the narrow structure amplitudes depend nonlinearly on the saturation parameter κ_s, with a maximum at $\kappa_s \approx 1$–2 [15]; the structure contrasts exhibit maxima when $\kappa_s \approx 0.5$–0.7.

The dependences of the half-widths of resonance narrow structures on the saturating field intensity are different for open and closed transitions: the half-width changes, respectively, as $\Gamma_w \approx \Gamma_n(1 + \kappa_s)$ and $\Gamma_w = \Gamma_n(1 + \kappa_s)/(1 + 2\kappa_s)$ [15]. Note that numerical calculations yield a close-to-linear rise in the structure (hole) width. The absence of the influence of saturating field intensity on the peak-structure width in the calculations under conditions of Figs 2, 3 is due to the insufficient spectral resolution. With a spectral resolution an order of magnitude higher, the calculations demonstrate narrowing of the peak structure with an increase in the saturating field intensity.

In a three-level system (Fig. 1a), a nonlinear resonance shape can be obtained from the system of equations (3)–(5) for a weak probe field in the approximation of first nonlinear strong-field corrections, large Doppler broadening ($\Gamma_{mn} \ll kv_T$) and frequency detunings $\Omega_\mu \ll kv_T$ and $\Omega \ll kv_T$ in the form

$$\frac{\alpha(\delta)}{\alpha_0 N_{nm}} = \sqrt{\pi}\frac{\Gamma_{mn}}{kv_T}\left\{1 - 2|G|^2\,\mathrm{Re}\left[\frac{\Gamma_m - A_{mn}}{\Gamma_m\Gamma_n}\frac{1}{2\Gamma_{mn} - i\delta}\right.\right.$$
$$\left.\left. - \frac{1}{2\Gamma_{mn} - \Gamma_m}\left(\frac{1}{2\Gamma_{mn} - i\delta} - \frac{1}{\Gamma_m - i\delta}\right)\right]\right\}, \qquad (8)$$

where $\delta = \varepsilon + \omega_{12} = \Omega_{20}^{\mu} - \Omega_{10}$.

In this case the nonlinear resonance profile is a sum of three Lorentzians with different amplitudes and widths, which are centred at the frequency difference $\delta = 0$. The first Lorentzian is the contribution of incoherent saturation of level populations, while the second and third Lorentzians are the contributions from coherent two-photon processes: step and two-photon absorption [13] in the three-level system.

For a closed transition (at $\Gamma_m = A_{mn}$), the contribution of the incoherent process to (8) is zero, and the nonlinear resonance profile is determined by the sum (interference) of the step and two-photon processes, which is a pure nonlinear interference effect in the three-level V scheme of the transition [13]. In this case the nonlinear resonance manifests itself as a hole near $\delta = 0$ (two-photon absorption dominates in this region) and two small-amplitude peaks, equally spaced from the line centre by $\delta = \pm\sqrt{3}\,\Gamma_m$. Similar nonlinear resonance profiles are observed in Fig. 3 at the values $\kappa_s \leqslant 0.02$ [curves (*1–4*)].

With an increase in the degree of transition openness (decrease in a_0), the peak amplitudes diminish and do not manifest themselves in the resonance profile at $a_0 \leqslant 0.9$. In this case, according to (8), the determining process in the formation of the resonance spectrum is incoherent saturation of level populations by a strong field, which creates a conventional hole with a half-width $2\Gamma_{mn}$.

2.3. $J = 1 \rightarrow J = 2$ transition

In the case of the $J = 1 \rightarrow J = 2$ transition (Fig. 1b), Eqns (1) and (2) yield the following system of equations for the level occupancies in the lower (n) and upper (m) states and for the polarisation coefficients R_{ik}, R^{μ}_{ik}, R^{s}_{ik}, r^{0}_{ik}, and $r^{\pm}_{ik}$:

$$\frac{d\rho^0_i}{dt} + \Gamma_n\rho^0_i = Q_i + \sum_k A_{ki}\rho^0_k + 2\,\mathrm{Re}\Big(i\sum_k G_{ik}R_{ki}\Big) + 2\,\mathrm{Re}\Big(i\sum_k G^{\mu}_{ik}R^{\mu}_{ki}\Big), \tag{9a}$$

$$\frac{d\rho^+_i}{dt} + [\Gamma_n + i(\varepsilon - (k_\mu - k)v)]\rho^+_i = \sum_k A_{ki}\rho^+_k + i\sum_k (G^{\mu}_{ik}R_{ki} - G_{ki}R^{\mu}_{ik} + G_{ik}R^{s}_{ki}); \tag{9b}$$

$$\frac{d\rho^0_k}{dt} + \Gamma_m\rho^0_k = Q_k + 2\,\mathrm{Re}\Big(i\sum_i G_{ki}R_{ik}\Big) + 2\,\mathrm{Re}\Big(i\sum_i G^{\mu}_{ki}R^{\mu}_{ik}\Big), \tag{10a}$$

$$\frac{d\rho^+_k}{dt} + [\Gamma_m + i(\varepsilon - (k_\mu - k)v)]\rho^+_k = i\sum_i (G_{ki}R^{\mu}_{ik} - G^{\mu}_{ik}R_{ki} - G_{ik}R^{s}_{ki}); \tag{10b}$$

$$\frac{dR_{ik}}{dt} + (\Gamma_{mn} - i\Omega_{ik})R_{ik} = -iG_{ik}(\rho^0_i - \rho^0_k) - iG^{\mu}_{ik}(\rho^+_k - \rho^+_i) + i(G_{il}r^0_{lk} - r^0_{il}G_{lk}) + i(G^{\mu}_{il}r^+_{lk} - r^+_{il}G^{\mu}_{lk}), \tag{11a}$$

$$\frac{dR^{s}_{ik}}{dt} + [\Gamma_{mn} - i(\Omega_{ik} - (\varepsilon - (k_\mu - k)v))]R^{s}_{ik} = -iG_{ik}(\rho^+_i - \rho^+_k) + i(G_{il}r^+_{lk} - r^+_{il}G_{lk}), \tag{11b}$$

$$\frac{dR^{\mu}_{ik}}{dt} + (\Gamma_{mn} - i\Omega^{\mu}_{ik})R^{\mu}_{ik} = -iG_{ik}(\rho^{+*}_i - \rho^{+*}_k) - iG^{\mu}_{ik}(\rho^0_i - \rho^0_k) + i(G_{il}r^-_{lk} - r^-_{il}G_{lk}) + i(G^{\mu}_{il}r^0_{lk} - r^0_{il}G^{\mu}_{lk}); \tag{11c}$$

$$\frac{dr^0_{ik}}{dt} + (\Gamma_{ik} + i\omega_{ik})r^0_{ik} = i(G_{il}R_{lk} - G_{lk}R^*_{li} + G^{\mu}_{il}R^{\mu}_{lk} - G^{\mu}_{lk}R^{\mu^*}_{li}) + \delta r^0_{ik}, \tag{12a}$$

$$\frac{dr^+_{ik}}{dt} + [\Gamma_{ik} + i(\omega_{ik} + (\varepsilon - (k_\mu - k)v))]r^+_{ik} = i(G^{\mu}_{il}R_{lk} - G_{lk}R^{\mu^*}_{li} + G_{il}R^{s}_{lk}) + \delta r^+_{ik}. \tag{12b}$$

Since the coefficients are Hermitian, only independent equations are written above. The subscripts i and k in Eqns (9)–(11) denote levels of different states, while the subscripts l and k denote the levels of the same state; $\Omega_{ik} = (\omega - \omega_{ik} - \boldsymbol{kv})$ and $\Omega^{\mu}_{ik} = (\omega_\mu - \omega_{ik} - \boldsymbol{k}_\mu\boldsymbol{v})$ are the detunings of field frequencies from the frequencies ω_{ik} of the transitions between the magnetic levels of different states, with allowance for the Doppler shift. The quantities ω_{ik} in Eqns (12) are the frequencies of the transitions between the magnetic levels of the same state and Γ_{ik} are the half-widths of these transitions. In the lower state, $i = 3$, $k = 1$, $l = 4–8$, and $\Gamma_{ik} = \Gamma_n$; in the upper state, $i = 6–8$, $k = 4–6$, $l = 1–3$, and $\Gamma_{ik} = \Gamma_m$. The terms δr^0_{ik} and δr^+_{ik} in Eqns (12) describe the spontaneous transfer of magnetic coherence from the upper state levels to the lower state. For the transition under consideration, $\delta r^{0,\pm}_{ik} = A^{83}_r r^{0,\pm}_{83} + A^{75}_r r^{0,\pm}_{75} + A^{64}_r r^{0,\pm}_{64}$, where the transfer rates are determined from [13] as $A^{83}_r = A^{64}_r = A_{mn}/\sqrt{6}$, and $A^{75}_r = A_{mn}/2$.

The steady-state systems of equations (9)–(12) were solved numerically, with variation in the level widths, branching ratio a_0, and light wave intensities (saturation parameters). The transition constants, Doppler linewidth, and integration conditions were the same as in the case of the $J = 0 \rightarrow J = 1$ transition. The shape of the probe-field absorption line was determined by an expression similar to (6), with allowance for the contribution from all transition components. The spontaneous decay probabilities of the magnetic sublevels, $A_{M'M}$, were assumed to be as follows [16]: $A_{21} = A_{-2-1} = A_{mn}$, $A_{11} = A_{-1-1} = 0.5A_{mn}$, $A_{10} = A_{-10} = 0.5A_{mn}$, $A_{01} = A_{0-1} = A_{mn}/6$, and $A_{00} = A_{mn}2/3$.

Calculations of the probe-wave saturated absorption spectra for this transition showed their dependence on the transition relaxation constants, branching ratio a_0, level splittings, field intensities, and the orientation of field polarisation planes. The characteristic spectra are shown in Fig. 4 for closed and open ($a_0 = 0.5$) transitions at linear (parallel and orthogonal) field polarisations in the absence of level splitting. In this case, a resonance in the form of a wide hole and narrow structure at the centre is formed on the Doppler absorption profile of the probe wave near the frequency $\Omega_\mu = 0$. The structure manifests itself as a peak for the closed transition [curves (*1,2*)] and as a hole for the open transition [curves (*3,4*)]. The parameters of the main hole and narrow structures depend differently on the orientation of field polarisations. In the case of closed transition, for orthogonally polarised fields, the amplitude and width of the main hole are smaller by a factor of about two, and the narrow peak amplitude is much larger than for parallel field polarisations. In addition, wide maxima are formed in the wings of the main hole [curve (*2*)]. For the open transition, a change in the polarisation directions barely changes the main-hole parameters; how-

ever the narrow structure amplitude is larger in the case of parallel field polarisations [curves(*3*, *4*)]. An increase in the degree of transition openness (a decrease in a_0), with other parameters fixed, leads to a rise in the width and a decrease in the amplitude of the main hole and the wing maxima. The narrow peak at the centre [curves (*1*, *2*)] is transformed into a narrow hole [curves (*3*, *4*)]; for fields with orthogonal and parallel polarisations the peak transformation occurs at $a_0 \approx 0.7$ and $a_0 \approx 0.95$, respectively.

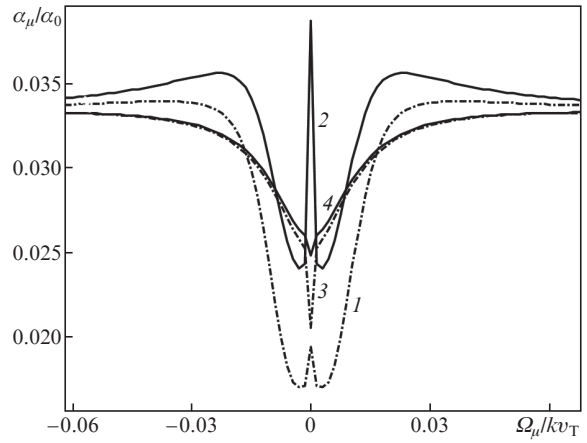

Figure 4. Shapes of the resonances on (*1*, *2*) closed and (*3*, *4*) open ($a_0 = 0.5$) transitions at (*1*, *3*) parallel and (*2*, *4*) orthogonal field polarisations ($\Omega_s = 0$, $\kappa_s = 1$, $\kappa_p = 0.001$, $\Gamma_n = 0.02\Gamma_m$).

Calculations showed that the amplitude and width of the main hole are determined by the relaxation constant Γ_{mn} and the values of field saturation parameters, whereas the narrow structure parameters are determined by the relaxation constant Γ_n of the lower level. A decrease in Γ_n causes a decrease in the width and a rise in the amplitude of the resonance narrow structure (peak and hole). A change in the relationship between the level relaxation constants (at $\Gamma_n \to \Gamma_m$) at a constant Γ_{mn} value leads to an increase in the absorption coefficient in the line wing, a rise in the amplitude and width of the main hole, and a decrease in the amplitudes and an increase in the widths of the resonance narrow structures.

An increase in the strong-wave intensity at any field polarisations leads to a rise in the amplitude and width of the main hole and the amplitudes of narrow structures; the broadening of the main hole is more pronounced at parallel field polarisations. In this case, the narrow hole width also increases, whereas the peak width barely changes.

The influence of the probe wave intensity on the nonlinear resonance shape manifests itself differently. For transitions of all types, at both parallel and orthogonal field polarisations, an increase in the probe wave intensity at saturation parameters $\kappa_p \leqslant \kappa_s$ leads to a decrease in the amplitude of the Doppler absorption profile and a decrease in the amplitudes and increase in the widths of both the main hole and narrow resonance structures. The resonance shape changes dramatically when the probe wave intensity exceeds the saturating wave intensity. In this case, at saturation parameters $\kappa_p > \kappa_s \sim 1$, a small resonance of opposite sign (EIT or EIA resonance) arises at the centre of the broadened narrow structure. Note that a similar transformation of EIA resonances into EIT resonances and vice versa was observed in [7].

Studies of the formation of probe-wave nonlinear absorption spectrum on the $J = 1 \to J = 2$ transition showed that the main contribution is from the two- and three-level V schemes, formed by the sublevels with a maximum magnetic number. Specifically these schemes determine the characteristic features of the nonlinear resonance spectrum, including the shapes of its narrow structures. The contributions of the transitions between other magnetic sublevels are much smaller. An example of the spectra of the contributions of individual transitions to the resonance in the absence of level splitting is shown in Fig. 5 for parallel field polarisations [the total profile is presented by curve (*1*) in Fig. 4]. The difference in the amplitudes of the Doppler pedestals of the spectra is due to the difference in the oscillator strengths, and the difference in the resonance shapes is related to the different degrees of openness of these transitions, because the transitions between the sublevels $M = \pm 1 \to M' = \pm 2$ are closed, whereas the transitions between other sublevels are open.

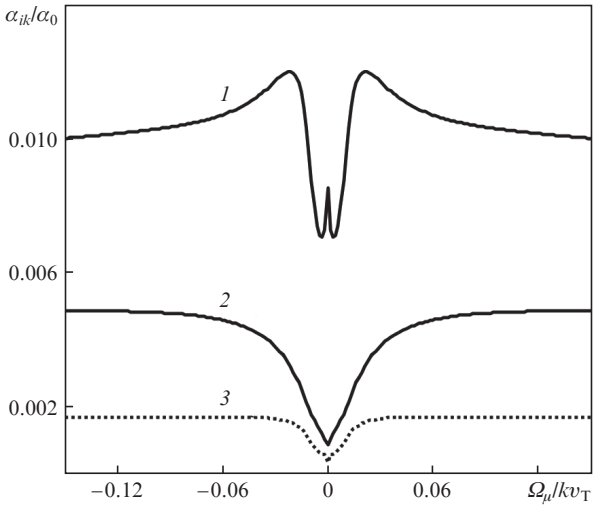

Figure 5. Spectra of the contributions of transitions between the magnetic sublevels (*1*) $M = \pm 1 \to M' = \pm 2$, (*2*) $M = 0 \to M' = \pm 1$, and (*3*) $M = \pm 1 \to M' = 0$ to the resonance at parallel field polarisations ($\Omega_s = 0$, $\Omega_H = 0$, $\kappa_s = 1$, $\kappa_p = 0.001$, $\Gamma_n = 0.02\Gamma_m$).

Calculations of the contribution of the magnetic coherence transfer from the upper state levels to the lower state, $\Delta\alpha_r/\alpha_0$ [contribution of the terms δr_{ik}^0 and δr_{ik}^+ in Eqns (12)], to the shape of saturated-absorption resonance showed that this contribution depends on the field saturation parameters, branching ratio a_0, level splitting, and field polarisation direction. The transfer contribution is maximum for a closed transition in the absence of level splitting. At parallel field polarisations, the transfer leads to a rise in the magnetic coherence of the lower levels and a decrease in the probe wave absorption near the line centre, whereas at orthogonal polarisations it decreases the level magnetic coherence and enhances the absorption. Figure 4 demonstrates that the maximum contribution of the magnetic coherence transfer to the resonance peak amplitude at orthogonal field polarisations is $\sim 10\%$, whereas at parallel polarisations it is smaller by a factor of more than two.

The calculations showed that the magnetic coherence transfer from the upper to lower levels cannot cause the forma-

tion of narrow (with a lower level width) structures in the nonlinear resonance spectrum, as was believed for a long time.

Splitting of the transition levels by a magnetic field leads to a change in the probe-wave saturated absorption spectra. The characteristic changes in the spectra with a level splitting Ω_H are shown in Fig. 6 for closed and open transitions at parallel field polarisations. For a closed transition (Fig. 6a), an increase in Ω_H leads to a decrease in the amplitude and width of the main hole and a rise in the peak amplitude. Maximum changes in these characteristics (by a factor of about two) are observed at small splittings ($\Omega_H \leqslant \Gamma_{mn}$). In the case of orthogonal field polarisations and $\Omega_H \leqslant \Gamma_{mn}$, an increase in the splitting Ω_H reduces by half the amplitudes of the peak and the main hole. The hole width does not change under these conditions. At splittings $\Omega_H > \Gamma_{mn}$, the resonance shapes become identical and independent of the orientation of field polarisations [curves (*3*, *4*)].

In the case of an open transition, the resonance shape undergoes also significant changes at small splittings: $\Omega_H \leqslant \Gamma_{mn}$ (Fig. 6b). An increase in Ω_H at arbitrary field polarisations leads to a decrease in the main-hole amplitude and width.

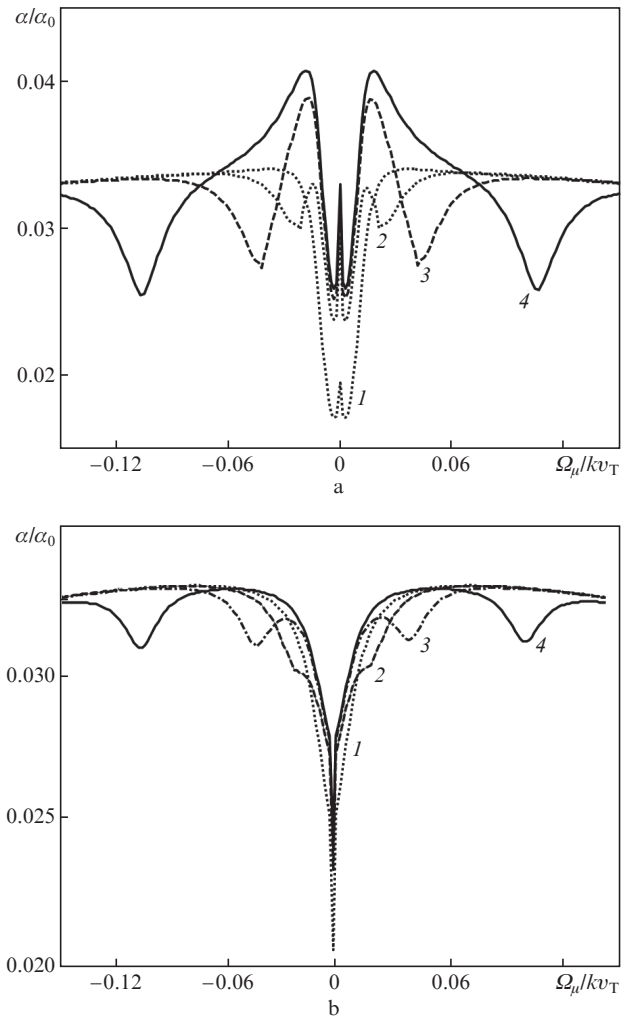

Figure 6. Shapes of the resonances at level splitting on (a) closed and (b) open ($a_0 = 0.5$) transitions at parallel field polarisations and $\Omega_H =$ (*1*) 0, (*2*) Γ_m, (*3*) $2\Gamma_m$, and (*4*) $5\Gamma_m$; $\Omega_s = 0$, $\kappa_s = 1$, $\kappa_p = 0.001$, and $\Gamma_n = 0.02\Gamma_m$.

The narrow structure amplitude decreases at parallel field polarisations (see Fig. 6b) and increases at orthogonal polarisations. At splittings $\Omega_H > \Gamma_{mn}$ the resonance shapes also become identical [curves (*3*, *4*)]. In this case, the absorption spectrum contains a resonance near $\Omega_\mu = 0$ and two resonances at the frequency $\Omega_\mu = \pm 2\Omega_H$.

Calculations showed the following: at any level splittings within the Doppler profile, the resonance near the line centre ($\Omega_\mu = 0$) in a system of two magnetic sublevels with a maximum number M is formed by fields with identical circular polarisations; this resonance manifests itself as a populational hole and a narrow coherent structure. The latter is shaped as a peak for a closed transition [Figs 6a and 4; curves (*1*)] and as a hole for an open transition [Figs 6b and 4; curves (*3*, *4*)]. The narrow structures (a peak or a hole) are formed due to the level population beatings in two-level transitions in the bichromatic field of light waves [11]. For a closed transition, as in [11], maxima are formed in the wings of populational hole [Fig. 6a; curves (*3*, *4*) and Fig. 4, curve (*1*)] due to the two-photon processes in the two-level system. For open transitions, there are no such structures in the wings [Fig. 4; curves (*3*, *4*)].

The resonances at frequencies $\Omega_\mu = \pm 2\Omega_H$, arising at level splitting (see Fig. 6), are formed by two-photon processes [13] and fields with opposite circular polarisations in the V schemes of the transition and have a populational character.

At small level splittings ($\Omega_H \leqslant \Gamma_{mn}$), an important contribution to the formation of resonance spectrum, as for the $J = 1$ transition [12], is made (along with the aforementioned processes) by the magnetic coherence of the levels (basically the lower state levels), induced by the field of a strong linearly polarised wave. The magnetic coherence of levels at parallel field polarisations weakens the absorption, while in the case of orthogonal polarisations it enhances the probe wave absorption (see [12] and references therein). The level splitting leads to destruction of level magnetic coherence. Correspondingly, the absorption is enhanced and weakened at parallel and orthogonal field polarisations, respectively (see Fig. 6). The contribution of the magnetic coherence to the resonance amplitude is maximum for a closed transition, depends on the strong-field saturation parameter, and amount to $\sim 35\%$ of the resonance amplitude at the parameters $\kappa_s \approx 1$.

3. Conclusions

The study of the saturated absorption spectra in the method of probe field of codirectional waves on transitions with level momenta $J = 0 \to J = 1$ and $J = 1 \to J = 2$ demonstrated their dependence on the level relaxation constants, value of level splitting, orientation of polarisations, and strong- and probe-wave intensities. The character of the spectra depends qualitatively on the degree of openness (branching ratio) of the atomic transition. It was shown that the specific features of saturated absorption spectra are formed mainly in the two-level and V schemes of the transition, formed by the sublevels with a maximum magnetic number M, and are determined by the level saturation and splitting, as well as the contributions from coherent processes: population beating and magnetic coherence of levels, induced by a strong-wave field. It is the specificity of relaxation of level population beatings that determines the form of narrow resonance structures: peak and hole for closed and open transitions, respectively. The contributions of the magnetic coherence of levels depend on the ori-

entation of strong- and probe-field polarisations and manifest themselves as additives; the main contribution is from the lower state levels. The contributions of the magnetic coherence transfer (from the upper levels to the lower state) to the resonance amplitude are small; they manifest themselves near the line centre.

To conclude, we should note that the width of the peak of narrow resonance structure on a closed transition may be smaller than the lower level width Γ_n. It is known that the relaxation constant Γ_n of moving atoms in the ground state is determined by their interaction time with optical fields (the average light beam flight time for an atomic ensemble); hence, the use of a gas of 'cold' atoms in experiments is expected to provide narrower and higher contrast peak resonance structures on closed transitions.

References

1. Aleksandrov E.B. *Sov. Phys. Usp*., **15**, 436 (1973) [*Usp. Fiz. Nauk*, **107**, 595 (1972)].
2. Saprykin E.G., Chernenko A.A., Shalagin A.M. *JETP*, **119**, 196 (2014) [*Zh. Eksp. Teor. Fiz.*, **146**, 229 (2014)].
3. Alzetta G., Gozzini A., Moi L., et al. *Nouvo Cim.*, **36**B, 5 (1976).
4. Arrimondo E., Orriols G. *Lett. Nouvo Cim.*, **17**, 333 (1976).
5. Akulshin F.M., Barreiro S., Lesama A. *Phys. Rev. A*, **57**, 2996 (1998).
6. Taichenachev A.V., Tumaikin A.M., Yudin V.I. *JETP Lett*., **69**, 819 (1999) [*Pis'ma Zh. Eksp. Teor. Fiz.*, **69**, 776 (1999)].
7. Kim S.K., Moon H.S., Kim K., et al. *Phys. Rev. A*, **61**, 063813 (2003).
8. Brazhnikov D.V., Taichenachev A.V., Tumaikin A.M., et al. *JETP Lett*., **91**, 625 (2010) [*Pis'ma Zh. Eksp. Teor. Fiz.*, **91**, 694 (2010)].
9. Goren C., Wilson-Gordon A.D., Rosenbluh M., et al. *Phys. Rev. A*, **67**, 033807 (2003).
10. Lazebnyi D.V., Brazhnikov D.V., Taichenachev A.V., et al. *JETP*., **121**, 934 (2015) [*Zh. Eksp. Teor. Fiz.*, **148**, 1068 (2015)].
11. Saprykin E.G., Chernenko A.A., Shalagin A.M. *JETP*, **123**, 205 (2016) [*Zh. Eksp. Teor. Fiz.*, **150**, 238 (2016)].
12. Saprykin E.G., Chernenko A.A. *JETP*, **127**, 189 (2018) [*Zh. Eksp. Teor. Fiz.*, **154**, 235 (2018)].
13. Rautian S.G., Smirnov G.I., Shalagin A.M. *Nelineinye rezonansy v spektrakh atomov i molekul* (Nonlinear Resonances in the Spectra of Atoms and Molecules) (Moscow: Nauka, 1979).
14. Saprykin E.G., Chernenko A.A., Shalagin A.M. *Opt. Spectrosc*., **113**, 530 (2012) [*Opt. Spektrosk.*, **113**, 530 (2012)].
15. Saprykin E.G., Chernenko A.A., Shalagin A.M. *Techn. Dijest 7-th Intern. Symp. MPLP-2016* (Novosibirsk, 2016) p. 232.
16. Sobel'man I.I. *Introduction to the Theory of Atomic Spectra* (Oxford: Pergamon Press, 1972; Moscow: Nauka, 1977).